



RESEARCH ARTICLE

Nonlinear interaction between APOE ϵ 4 allele load and age in the hippocampal surface of cognitively intact individuals

Gerard Martí-Juan¹  | Gerard Sanroma-Guell² | Raffaele Cacciaglia^{3,4,5} |
 Carles Falcon^{3,4,6} | Grégory Operto^{3,4,5} | José Luis Molinuevo^{3,4,5,7} |
 Miguel Ángel González Ballester^{1,8} | Juan Domingo Gispert^{3,4,6,7}  | Gemma Piella¹ |
 The Alzheimer's Disease Neuroimaging Initiative | The ALFA Study

¹BCN MedTech, Departament de Tecnologies de la Informació i les Comunicacions, Universitat Pompeu Fabra, Barcelona, Spain

²German Center for Neurodegenerative Diseases (DZNE), Bonn, Germany

³Barcelonaβeta Brain Research Center (BBRC), Pasqual Maragall Foundation, Barcelona, Spain

⁴Hospital del Mar Medical Research Institute (IMIM), Barcelona, Spain

⁵Centro de Investigación Biomédica en Red de Fragilidad y Envejecimiento Saludable (CIBERFES), Madrid, Spain

⁶Centro de Investigación Biomédica en Red de Bioingeniería, Biomateriales y Nanomedicina (CIBERBBN), Madrid, Spain

⁷Universitat Pompeu Fabra, Barcelona, Spain

⁸ICREA, Barcelona, Spain

Correspondence

Juan Domingo Gispert, Centro de Investigación Biomédica en Red de Fragilidad y Envejecimiento Saludable (CIBERFES), Madrid, Spain.
 Email: jdgpert@barcelonabeta.org

Gemma Piella, BCN MedTech, Departament de Tecnologies de la Informació i les Comunicacions, Universitat Pompeu Fabra, Barcelona, Spain.
 Email: gemma.piella@upf.edu

Funding information

"la Caixa" Foundation, Grant/Award Number: LCF/PR/GN17/50300004; Ministry of Business and Knowledge of the Catalan Government, Grant/Award Number: 2017-SGR-892; Spanish Ministry of Economy and Competitiveness, Grant/Award Number: MDM-2015-0502; Spanish Ministry of Science, Innovation and Universities, Grant/Award Number: RYC-2013-13054

Abstract

The ϵ 4 allele of the gene Apolipoprotein E is the major genetic risk factor for Alzheimer's Disease. APOE ϵ 4 has been associated with changes in brain structure in cognitively impaired and unimpaired subjects, including atrophy of the hippocampus, which is one of the brain structures that is early affected by AD. In this work we analyzed the impact of APOE ϵ 4 gene dose and its association with age, on hippocampal shape assessed with multivariate surface analysis, in a ϵ 4-enriched cohort of $n = 479$ cognitively healthy individuals. Furthermore, we sought to replicate our findings on an independent dataset of $n = 969$ individuals covering the entire AD spectrum. We segmented the hippocampus of the subjects with a multi-atlas-based approach, obtaining high-dimensional meshes that can be analyzed in a multivariate way. We analyzed the effects of different factors including APOE, sex, and age (in both cohorts) as well as clinical diagnosis on the local 3D hippocampal surface changes. We found specific regions on the hippocampal surface where the effect is modulated by significant APOE ϵ 4 linear and quadratic interactions with age. We compared between APOE and diagnosis effects from both cohorts, finding similarities between APOE ϵ 4 and AD effects on specific regions, and suggesting that age may modulate the effect of APOE ϵ 4 and AD in a similar way.

Abbreviations: AD, Alzheimer's Disease; ADNI, Alzheimer's Disease Neuroimaging Initiative; ALFA, Alzheimer and Families; CN, cognitively normal; DX, diagnosis; HE, heterozygotes; HO, homozygotes; MCI, mild cognitive impairment; NC, noncarriers.

This is an open access article under the terms of the Creative Commons Attribution-NonCommercial License, which permits use, distribution and reproduction in any medium, provided the original work is properly cited and is not used for commercial purposes.

© 2020 The Authors. *Human Brain Mapping* published by Wiley Periodicals LLC.

KEYWORDS

Alzheimer's disease, APOE, cognitively intact, hippocampus, multivariate analysis

1 | INTRODUCTION

Alzheimer's Disease (AD) is a neurodegenerative disorder characterized by progressive decline in multiple cognitive domains and severe brain atrophy. AD affects millions of elderly people worldwide (Alzheimer's Association, 2018) and despite major research efforts to halt or reverse the degenerative process, it has no cure. The major genetic risk factor for AD is the Apolipoprotein E (APOE) $\epsilon 4$ allele (Saunders et al., 1993). The main function of APOE in the brain is cholesterol transport (Saunders et al., 1993), and it modulates various pathways related to AD pathogenesis, including $A\beta$ clearance and neuroinflammation (Zhao, Liu, Qiao, & Bu, 2018). APOE has three different alleles in humans ($\epsilon 2$, $\epsilon 3$, and $\epsilon 4$), with the latter (APOE $\epsilon 4$) being linked to increased risk of AD and to an earlier disease onset in a gene dose-dependent manner (Liu, Kanekiyo, Xu, & Guojun, 2013). The investigation of brain imaging phenotypes related to APOE $\epsilon 4$ in cognitively intact individuals provides the opportunity to reveal early pathological changes.

The impact of APOE- $\epsilon 4$ allele load in preclinical subjects can be studied using different neuroimaging biomarkers (Chételat & Fouquet, 2013). For example, decreased cerebral metabolism as well as increased $A\beta$ deposition have been observed in cognitively unimpaired individuals in association with the number of $\epsilon 4$ alleles (Reiman et al., 2005, 2009). Concerning the impact on brain morphology Fouquet, Besson, Gonneaud, La Joie, and Chételat (2014) found in their meta-analysis that the results are "rather discrepant", suggesting that the effect of the allele load on brain morphology is subtle, and difficult to detect. Yet, capitalizing on a cognitively healthy at-risk cohort with a high number or $\epsilon 4$ -homozygous individuals, a recent study found similar gene-dose effects in gray matter volumes of cognitively healthy participants (Cacciaglia et al., 2018).

The hippocampus is one of the earliest structures undergoing neurodegeneration in the initial stages of the Alzheimer's continuum (Pievani et al., 2011), and it has been used for diagnosis and early prediction of AD (Sanroma et al., 2017). Longitudinal studies confirmed that hippocampal atrophy can appear in asymptomatic subjects at risk of familial AD (Fox et al., 1996). It was also shown that APOE $\epsilon 4$ allele load is associated with the hippocampus morphology, even in cognitively healthy subjects. A difference in the volume of the right hippocampus was found between APOE $\epsilon 4$ carriers and noncarriers (O'Dwyer et al., 2012). This difference in volume was also detected by Lind et al. (2006), who found it more profound in younger carriers (<65), and by Tondelli et al. (2012), who reported right hippocampus changes to be predictive of AD. However, other studies claim that the left hippocampus is more predictive and presents the most significant effects (Csernansky

Highlights

- The effect of APOE $\epsilon 4$ and other factors on hippocampal morphology in cognitively impaired and healthy subjects, and its interaction with age was analyzed.
- Additive, dominant, recessive, and AD odds risk models for APOE were used.
- Significant interactions between APOE and age on cognitively healthy subjects on hippocampal surface were found.
- Similarities between APOE effects on cognitively healthy subjects and the disease effect were found. Strong similarities between interaction effect of APOE and age on cognitively healthy subjects and interaction effect between diagnosis and age were also captured.

et al., 2005). Shi et al. (2014) proposed a multivariate shape analysis of the hippocampus, studying the genetic influence of APOE in patients at different stages of AD. They found differences between carriers and noncarriers in the left hippocampus for cognitively normal (CN) and mild cognitive impaired (MCI) patients, and for demented patients. In a more recent work, Dong et al. (2019) used the same method as in Shi et al. (2014) on a cohort of cognitively unimpaired subjects. Results found a more pronounced effect on the left hippocampus. Other studies found no remarkable volumetric differences between carriers and noncarriers (Hostage, Choudhury, Doraiswamy, & Petrella, 2013; Protas et al., 2013), whereas more recent ones found differences in hippocampal subfields, but only for early onset AD (Parker et al., 2019). The seemingly contradictory results of those studies show that the effect of APOE $\epsilon 4$ load on healthy brains is still not clear. This could be due to several reasons: the use of different methodologies, the low signal of the effect, which makes it difficult to detect it, or the modulation of the effect by other factors, which could make such effect non-homogeneous across subjects.

Some studies suggest an interaction between age and APOE $\epsilon 4$ allele load effect (Tuminello & Han, 2011), arguing that APOE effect on the brain could depend on the age of the subject. Mueller and Weiner (2009) found significant differences in hippocampal volumes between carriers and noncarriers, and effects of age in different subfields (CA3 and DG) of the hippocampus. In a previous work (Mueller, Schuff, Raptentsetsang, Elman, & Weiner, 2008), they had found an effect of APOE $\epsilon 4$ in healthy older subjects, but not in younger. Kate et al. (2016) found an interaction with gray matter volume values, and

Cacciaglia et al. (2018) showed significant interactions between APOE homozygotes and age on the volume of the right hippocampus, as well as in other brain structures.

Previously described interactions are based on volumetric data, so more subtle morphology changes unrelated to volume difference might be missed. Shape analysis complements volumetric analysis and can identify and locate subtle regional abnormalities on brain structures, even if there are no changes in volume. Many different approaches have been proposed to capture and study morphological shape changes on brain structures (Nitzken et al., 2014; Shen, Cong, & Inlow, 2017; Zhang & Golland, 2016). Surface-based shape representation on using spherical harmonics as a parametric descriptor (SPHARM) (Styner et al., 2006) is a common approach for subcortical regions, including the hippocampus (Shen, Ford, Makedon, & Saykin, 2003; Shi et al., 2007; Styner, Lieberman, Pantazis, & Gerig, 2004; Zhao et al., 2008), with recent works that also incorporate subfield information to the analysis (Cong et al., 2015; Inlow et al., 2016). Another approach is to use hippocampal radial distance (Thompson et al., 2004), relating surface points to a medial curve of each object (Apostolova et al., 2010; Bouix, Jens, Pruessner, & Siddiqi, 2005; Chung, Worsley, Nacewicz, Dalton, & Davidson, 2010; Costafreda et al., 2011; Morra et al., 2009). Deformation-based representations, where descriptors of the shape are defined by the deformation obtained by registering the image to a desired template (Joshi, Xie, Kurtek, Srivastava, & Laga, 2016; Kim, Valdes-Hernandez, Royle, & Park, 2015), are also frequently used. A popular framework for this approach is the large deformation diffeomorphic metric mapping (Beg, Miller, Trounev, & Younes, 2005; Miller, Trounev, & Younes, 2006), which uses diffeomorphic transformations to parametrize the different shapes and map the template to each subject. Several methods based on this framework have been proposed and applied in subcortical brain structures (Durrleman et al., 2014; Li, Gong, & Tang, 2017; Miller et al., 2015; Singh et al., 2014; Vaillant, Qiu, Glaunès, & Miller, 2007; Younes, Albert, & Miller, 2014), including the hippocampus (Cury et al., 2018; Qiu et al., 2009; Tang et al., 2016). Other different methods have been proposed, such as Bayesian-based analysis (Gori et al., 2017; Gutiérrez, Gutiérrez-Peña, & Mena, 2019), or spectral matching (Shakeri et al., 2016). Some studies also incorporate longitudinal shape change onto the analysis, to capture and analyze shape trajectories along time (Bône, Colliot, & Durrleman, 2018; Cury et al., 2019; Miller et al., 2015). Recently, software tools allowing for easy shape processing and analysis have been made available, such as ShapeWorks (Cates, Elhabian, & Whitaker, 2017), implementing a particle-based model without parametrizations, or Deformetrica (Bône, Louis, Martin, & Durrleman, 2018), using the large deformation diffeomorphic metric framework for various functionalities. Comparison and validation of such tools and methods show that some performance inconsistencies still remain (Gao, Riklin-Raviv, & Bouix, 2014; Goparaju et al., 2018; Madan & Elizabeth, 2017), and research on the field is still expanding.

Our objective is to study effects and interactions of APOE allele load on the hippocampal morphology of cognitively unimpaired

subjects at risk of AD. To that end, we analyze linear and nonlinear interactions between APOE $\epsilon 4$ allele load and age on the geometric differences on the surfaces of normalized shapes. We present our results on two cohorts: (a) The ALFA cohort (Molinuevo et al., 2016), composed of cognitively healthy participants enriched with individuals at higher genetic risk for AD, and (b) the ADNI cohort (Mueller et al., 2005), containing a mixture of healthy and cognitively impaired subjects with different degrees of AD pathology. The reason of analyzing this second population is twofold. First, to study whether the APOE $\epsilon 4$ effect in the first cohort has some resemblance or affinity to the AD effect in the second cohort; that is, we want to explore if the effect of different APOE allele load is related to the effect produced by the disease on hippocampal shape. And second, to evaluate whether APOE $\epsilon 4$ allele load has a similar effect in both cohorts. We segment the hippocampus and use a diffeomorphic registration approach to generate the corresponding meshes. We use multivariate statistical shape analysis to detect subtle surface changes that could be undetectable when analyzing structural volume or gray matter density. We analyze the effects of multiple factors on hippocampal morphology, namely, APOE, age, sex, and diagnosis (when applicable), study linear and nonlinear interactions between age, APOE and diagnosis, and we quantified the similarity between different effects on the two populations. The proposed shape analysis method allows visualizing both the magnitude and the direction of the effect on the whole surface of the hippocampus, thus providing new insight about the corrected effect of APOE $\epsilon 4$ (and other factors) on hippocampal morphology.

2 | METHODS

In this section, we detail the pipeline of our method to extract the hippocampal meshes from the imaging data and the experimental design. All code to reproduce the pipeline and experiments described here can be found in the repository of the project.¹

2.1 | Subjects

We analyzed two cohorts:

1. Alzheimer and FAMILIES (ALFA) study (Molinuevo et al., 2016), a genetically enriched dataset of cognitively healthy subjects with high proportion of $\epsilon 4$. These are pooled between noncarriers (NC), heterozygotes (HE), carrying one copy of the allele, and homozygotes (HO), carrying two copies. This cohort is ideal to study early pathophysiological effects of AD and the possible effects of APOE $\epsilon 4$ in the preclinical phase of the disease. Five hundred and eighteen subjects from the cohort were used for this study. Magnetic resonance imaging (MRI) was conducted with a 3T General Electric scanner (GE Discovery MR750 W). Structural 3D high-resolution T1-weighted images were collected using a fast spoiled gradient-echo sequence implementing the following parameters: voxel

size = 1 mm³ isotropic, repetition time = 6.16 ms, echo time = 2.33 ms, inversion time = 450 ms, matrix size = 256 × 256 × 174, and flip angle = 12°.

2. Alzheimer's Disease Neuroimaging Initiative (ADNI) (Mueller et al., 2005). ADNI is one of the largest longitudinal public dataset on AD, containing not only MRI but also other imaging modalities and genetic information, among others. One thousand and sixteen subjects from the main study of ADNI were used for this work, in order to detect affinities between the effect of AD onto hippocampus shape and the effect of APOE allele load in cognitively healthy subjects from the ALFA dataset, and to assess the effect of APOE in patients at different stages of the disease. Structural 3D high-resolution T1-weighted MRI scans were available for every subject. ADNI is a multisite study, so there are differences in MRI acquisition between scans. For this reason, in all ADNI tests, we included site as a covariate to correct for possible site differences (Section 2.3). Further information on image acquisition for the ADNI scans used in this work can be found in Jack et al. (2010).

2.2 | Pipeline

Our data processing pipeline consists of four stages: hippocampus segmentation on the MRI, image registration to a common template, mesh generation, and shape normalization. Figure 1 shows the full pipeline.

1. Hippocampus segmentation: We used a multi-atlas segmentation approach with joint label fusion and corrective learning (Wang & Yushkevich, 2013) to segment the hippocampi. We chose this algorithm, implemented in the ANTs library (Avants, Epstein, Grossman, & Gee, 2008), because of its top performance in various segmentation challenges (Wang & Yushkevich, 2013) and good performance when compared to other segmentation methods (Dill, Franco, & Pinho, 2015). As atlas, we used 15 segmented MRI scans from the ADNI database. The hippocampus segmentations of the atlases, provided by ADNI, were computed using a semi-automatic hippocampal volumetry method (Hsu et al., 2002). The 15 atlas were selected so that they spanned a wide hippocampal shape variability (Sanroma, Wu, Gao, & Shen, 2014).
2. Image registration: We nonrigidly registered each subject's image and its corresponding segmentation to a template image (MNI152) and its corresponding ground truth hippocampus segmentation using the symmetric diffeomorphic normalization approach (Avants et al., 2008) implemented in ANTs library. We used two channels, equally weighted, to jointly register the subject image to the template image and the hippocampus segmentation of the subject to the template segmentation. This allowed us to obtain a more precise registration between each image and the template, while ensuring that the corresponding segmentations match well. The registration generates a deformation field for each subject.
3. Mesh deformation: We used the segmentation from the template image to build a template mesh, using the marching cubes

algorithm (Lorensen & Cline, 1987), giving more vertex density to regions with higher curvature. The deformation fields obtained from the previous registration stage were used to warp the template mesh to each subject space. This procedure ensures that the generated meshes have vertex and triangle correspondences, which directly facilitates the downstream statistical analysis.

4. Shape normalization: After obtaining all the individual meshes, we processed them to remove undesired variation. Since we are interested in shape changes, we aligned the meshes using Procrustes analysis (Gower, 1975) to compensate rotational and translational variations not already removed in the registration stage. Unlike the normal Procrustes analysis, scaling was not performed so as to preserve the size information. Even if some meshes present large atrophied and/or missing regions, with the point-to-point correspondence obtained in the previous step, they are directly comparable and hence their associated deformations can be captured.

We also conducted both an automatic and a manual quality control to detect segmentation and mesh extraction errors. First, we computed the volumes of each mesh, discarding the meshes that were outliers. Then, we did a manual check of all the obtained meshes and discarded those that had obvious visual errors. In total, we removed 39 scans from the original ALFA dataset and 47 scans from ADNI, resulting in 479 and 969 total scans, respectively. Table 1 shows the demographic characteristics for both cohorts.

2.3 | Statistical analysis

Using the mean mesh (after Procrustes) as a reference mesh, we defined $y_i = (y_{i0}, y_{i1}, y_{i2}) \in \mathbb{R}^3$ as the vector of the residuals between the i -th vertex coordinates of the subject mesh and the reference mesh. The choice of reference is irrelevant for the analysis, since the bias term in the regression below ensures that the origin corresponds to the population mean for each vertex.

The model at each vertex i for each dimension j is a multiple regression model with interaction terms, of the form:

$$y_{ij} = \alpha_j + \sum_{k \in \varphi} \beta_{kj} c_k + \varepsilon_j \text{ for } j = 0, 1, 2,$$

where α is the intercept, β_{kj} is the coefficient for covariate or interaction c_k , φ is the set of indices of covariates and their interactions, and ε is the error term. Left and right hippocampus were analyzed separately.

APOE $\varepsilon 4$ status was included as a covariate. We considered an additive model as well as dominant and recessive models. For the additive model, the allele variable indicated the number of copies of the $\varepsilon 4$ allele (e.g., 0, 1, or 2). For the dominant and recessive models, we used binary (aka dummy) variables. In the dominant model, the variable coded the presence or absence of the $\varepsilon 4$ allele (e.g., 0 indicating zero copies of the risk allele and 1 indicating one or two copies). In

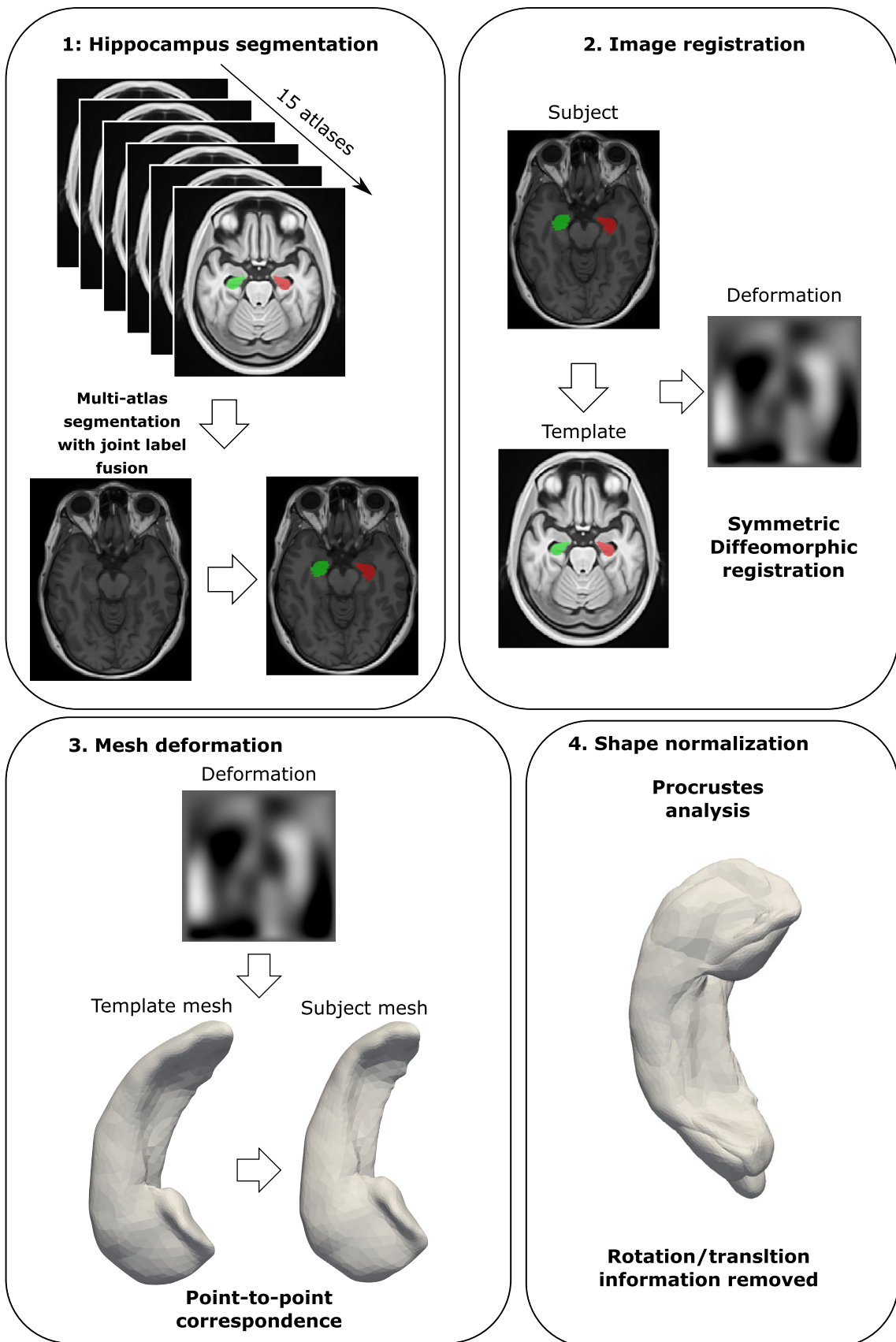


FIGURE 1 Outline of the processing pipeline

TABLE 1 Demographics characteristics for the cohorts used in the article

APOE $\epsilon 4$	Noncarriers	Heterozygotes	Homozygotes	Total	Statistics
ALFA					
Number	234	187	58	479	—
Age	57.88 \pm 7.55	58.55 \pm 7.41	53.93 \pm 6.14	57.66 \pm 7.46	$F = 5.69, p = .017$
Education	13.62 \pm 3.66	13.81 \pm 3.48	13.59 \pm 3.35	13.69 \pm 3.55	$F = 0.03, p = .852$
Male/female	88/146	87/100	23/35	198/281	$\chi^2 = 3.48, p = .170$
MMSE	28.96 \pm 1.14	29.14 \pm 1.00	29.1 \pm 1.06	29.05 \pm 1.08	$F = 1.78, p = .183$
Diagnosis	CN	MCI	AD	Total	Statistics
ADNI					
Number	281	475	213	969	—
Noncarriers	203	231	70	504	—
Heterozygotes	71	189	100	360	—
Homozygotes	7	55	43	105	—
Age	75.25 \pm 5.31	74.13 \pm 7.52	74.91 \pm 7.49	74.62 \pm 6.95	$F = 0.56, p = .456$
Education	16.15 \pm 2.78	15.76 \pm 2.65	14.84 \pm 3.14	15.67 \pm 2.99	$F = 22.97, p > .001$
Male/female	144/137	298/177	109/104	551/418	$\chi^2 = 13.11, p = .001$
MMSE	29.05 \pm 1.07	27.2 \pm 1.82	23.29 \pm 2.06	26.88 \pm 2.67	$F = 1,230, p < .001$

Notes: Age and education presented as average and standard deviation, in years.

Abbreviations: AD, Alzheimer's disease; CN, cognitively normal; MCI, mild cognitive impairment; MMSE, mini-mental state examination.

the recessive model, the variable coded the presence or absence of two copies of the $\epsilon 4$ allele (e.g., 0 corresponding to zero or one copies of the risk allele).

The previous models assume that the AD risk on APOE $\epsilon 4$ is linear with the number of alleles, and they do not account for the potential reduced risk of APOE $\epsilon 2$, which has been well documented (Genin et al., 2011; Liu et al., 2013). For this reason, we also used a model that includes the associated AD risk for each allele pair. AD risk was included from (Reiman et al., 2020), which defined AD risk for the different APOE allele pairs on a cohort of over 5,000 neuropathologically characterized AD and control participants. We encoded the odds ratio (OR) of AD risk of each allele pair compared to $\epsilon 3\epsilon 3$, and applied a logarithm to linearize the risk values and normalize the residuals. Table 2 shows the distribution of allele pairs over both datasets.

We also included, as covariates, age, sex, and years of education. In the experiments that included ADNI subjects, we also included diagnosis (DX) and site, a variable that accounts for the different sites where images were captured. Age was centered at its respective mean to limit the effects of multicollinearity when evaluating the quadratic effects.

For the statistical analysis, we combined the univariate T statistics over all coordinates on a single statistic, by finding the maximum over all possible linear combinations. This maximum is the Hotelling's T statistic (Hotelling, 1931). This final T-statistic was then used to test for significance of the effects. As the number of vertices was large, we corrected for multiple comparisons to remove false positives and obtained significant clusters of vertices over the hippocampal surface. We applied family-wise error correction with random field theory to account for spatial correlation (Hayasaka, Phan, Liberzon, Worsley, &

TABLE 2 APOE Allele pair counts for the cohorts used in this article

	Noncarriers			HE		HO	Total
	$\epsilon 2\epsilon 2$	$\epsilon 2\epsilon 3$	$\epsilon 3\epsilon 3$	$\epsilon 2\epsilon 4$	$\epsilon 3\epsilon 4$	$\epsilon 4\epsilon 4$	
ADNI	3	67	434	22	338	105	969
ALFA	7	97	130	38	149	58	479
Total	10	164	564	60	487	163	1,448

Abbreviations: HE, heterozygotes; HO, homozygotes.

Nichols, 2004). We selected only significant clusters with a number of vertices larger than a given threshold to further remove false positives. We set that threshold to 20.

2.4 | Experimental design

We defined three different settings for our experiments, depending on the data used. Alignment of the meshes prior to analysis, as described in Section 2.2, was done independently for each of the settings. For each setting, we analyzed a model with no interaction terms (we refer to this model as the base model), and several models with the specified interaction terms. Each model was evaluated using the different APOE encodings previously mentioned:

- Case I: the analysis was performed on the ALFA cohort. We added to the base model the interactions terms between age (linear and squared) and APOE.

- Case II: the analysis was performed on the ADNI cohort. We added to the base model the diagnosis information and interaction terms between age (linear and squared) and APOE, age and diagnosis, and diagnosis and APOE.
- Case III: the analysis was performed on the healthy subjects of the ADNI cohort. Despite the low amount of samples and small proportion of homozygotes, we wanted to test for interactions between age (linear and squared) and APOE to see if the effect of the interactions could be compared to the effect obtained in the ALFA experiments.

We also considered a fourth setting, which jointly analyzed both cohorts, considering ALFA subjects to be a new site and having CN as diagnosis. We repeated all the previous tests for this joint dataset. However, results were not included in the main text as no significant regions were observed; they can be found on Tables S1 (base model) and S2 (interaction model between APOE and age). All the models and experiments were implemented in MATLAB using the SurfStat toolbox (Worsley et al., 2009).

2.5 | Visualization and effect comparison

For better visualization of the effect of each factor and interaction over the hippocampal surface, we defined a 3D vector for each vertex i and effect $k \in \varphi$: $b_i^k = (\beta_{k0}, \beta_{k1}, \beta_{k2})$. Note that this vector does not represent deformations, but rather the effect of the indicated factor on that vertex (i.e., point of the surface). We defined the color of the effect depending on whether it is a contraction (dark violet, negative values) or expansion (light yellow, positive values) displacement, with respect to the normal of the template surface at that mesh point, and the strength of the effect. Note that, given this criteria, some artifacts could appear in the coloration depending on whether the effect is close to being orthogonal to the normal. In the representation shown in the figures, arrow length and size indicate a stronger effect. The arrows are distributed equally over the vertices for an easier visualization.

To quantitatively compare and quantify the similarity between the results of two different effect maps, we used cosine similarity. For two vector effects $b1$ and $b2$ located on the same vertex i , but coming from different experiments:

$$S(b1, b2) = \frac{b1 \cdot b2}{|b1| |b2|}$$

This metric was selected for effect comparison because it allows us to highlight and quantify the similarity of the effect direction over the surface. We do not want to compare the strength of the effect, which, given the differences between cohorts, could greatly vary and be misleading. The cosine similarity was rescaled to lie between 0 (i.e., vectors have opposite direction) and 1 (i.e., vectors have the same direction), with 0.5 indicating orthogonality between the two vectors.

To test the statistical significance of the similarity, we performed a randomization test, which corrects for multiple comparison. We first created a distribution of similarities for a large number K of pairs of random vectors $k = (k_0, k_1, k_2)$, with $k \sim \mathcal{N}(0, 1)^3$. We set $K = 100,000$. Then, we assessed, for each similarity value, its percentile over the distribution, obtaining the corresponding p -value. Finally, we selected clusters of vertices with $p < .05$, removing those with less than 20 vertices to further reduce false positives. In this way, we can detect relevant local areas where there is a strong similarity.

We compared similarity of effects obtained between ALFA and ADNI base models, ALFA interaction and ADNI base models, and ALFA and ADNI interaction models. We also wanted to assess if detected APOE effects and interactions in ALFA were similar to those in ADNI. For this reason, we compared the similarity between ALFA and healthy patients in ADNI, base and interaction models, and ALFA and ALFA plus ADNI, base and interaction models.

3 | RESULTS

3.1 | ALFA dataset

Table 3 summarizes the main results for all the experiments done on the ALFA cohort. Results are shown for the base model, a model with a linear interaction term between APOE and age, and another with a linear and squared interaction. The “Results” column shows the general statistical results, whereas the “Cluster analysis” column shows information about the detected clusters on the hippocampal surface after correction. More than one line for a single test shows that more than one significant cluster was detected for that test.

For the base model, Table 3 (upper part) summarizes the effect of each covariate (age, sex, years of education and APOE) over the mesh, for the base model without interactions, and its detected significant clusters. No significant clusters were found for any of the APOE contrasts. Figure 2 shows the effect of selected covariates over the hippocampus mesh. We can observe strong effects for age, with large association with surface expansion at zones on the head and tail of the hippocampus, and contraction in the body, and sex, with a general contraction effect that is largely associated to intra-cranial volume (as we did not correct for it in the preprocessing to not remove relevant information). For the linear interaction model, Table 3 (middle part) summarizes the effects in the model with a linear interaction between APOE and age, focusing on additive, dominant, and APOE OR effects, and the differences between homozygotes and noncarriers. Corresponding significant clusters are also included. For the effects of the APOE and age interaction between HO and NC groups, a significant cluster associated to a linear expansion effect was detected in the head of both hippocampus. Figures S3 and S4 show the effects of the APOE and age interaction, between HO and NC groups and the magnitude of the vector of the corrected response

TABLE 3 Results obtained on the ALFA cohort for base, linear interaction, and squared interaction models

	Test	Results			Cluster analysis			
		Hipp	Avg. <i>T</i>	Max. <i>T</i>	<i>N</i>	<i>P</i> _{peak}	<i>P</i> _{cluster}	
Base model	Age	R	1.34	9.64	2,121	<.001	<.001	
		L	1.24	8.41	1898	<.001	<.001	
	Sex	R	2.23	12.17	2,605	<.001	<.001	
		L	2.28	13.15	2,438	<.001	<.001	
	Years ed.	R	0.58	2.75	—	—	—	
		L	0.61	3.04	—	—	—	
	APOE (additive)	R	0.55	2.4	—	—	—	
		L	0.63	3.1	—	—	—	
	APOE (dominant)	R	0.56	2.38	—	—	—	
		L	0.64	3.12	—	—	—	
	APOE (recessive)	R	0.61	2.61	—	—	—	
		L	0.63	2.89	—	—	—	
	APOE (log(OR))	R	0.58	2.62	—	—	—	
		L	0.61	2.96	—	—	—	
	Linear int. model	APOE (add)×age	R	0.68	4.02	50	.093	.012
			L	0.68	4.12	172	.068	.006
APOE (Dom)×age		R	0.69	4.09	48	.079	.016	
		L	0.67	3.88	135	.141	.015	
APOE (HO > NC)×age		R	0.72	4.16	50	.06	.02	
		L	0.68	4.30	150	.038	.005	
APOE (log(OR))×age		R	0.69	3.67	—	—	—	
		L	0.67	4.08	—	—	—	
Squared int. model		APOE (add)×age	R	0.85	4.57	260	.015	.001
			L	0.7	3.17	—	—	—
	APOE (add)×age ²	R	0.78	4.67	270	.01	<.001	
		L	0.65	3.14	—	—	—	
	APOE (HE > NC)×age	R	0.92	4.23	313	.045	.004	
		L	0.78	3.19	—	—	—	
	APOE (HE > NC)×age ²	R	0.82	4.31	333	.037	.002	
		L	0.7	3.18	—	—	—	
	APOE (log(OR))×age ²	R	0.81	4.69	86	.009	.003	
		L	0.66	3.24	44	.012	.004	

Notes: General test results and information about significant clusters that survived correction are included. Results are divided by model (base, linear interaction or squared interaction). Hipp indicates left (L) or right (R) hippocampus. Max. and Avg. *T* are the maximum and average Hotelling's *T* statistic over all vertices, respectively. *XX* > *YY* indicates the comparison used for that specific test. For the cluster analysis after correction, *N* is the number of vertices of the significant cluster. *P*_{peak} and *P*_{cluster} are the random field corrected *p*-values for the peak point and the whole cluster, respectively. Only clusters with *N* > 20 and *P*_{cluster} < .05 are included.

Abbreviations: Add, additive; Dom, dominant; OR, Odds ratio of AD risk; Rec: recessive.

variable *y* in that region, compared to age, for each of the three APOE allele groups, respectively.

For the squared interaction model, Table 3 (lower part) shows the effects of the squared interaction between APOE OR and age, as well as the effects of the additive, dominant and AD risk interaction terms with age and squared age, and the information about the surviving

clusters in the interaction models. Figure 3 shows three different clusters where a significant expansion can be found on two different clusters, two on the head of the hippocampus, and a smaller one on the hippocampal tail. The first two clusters also appear on an additive interaction model (Supporting Information S5). A similar region appears when comparing HE vs NC. Figure 3 also shows

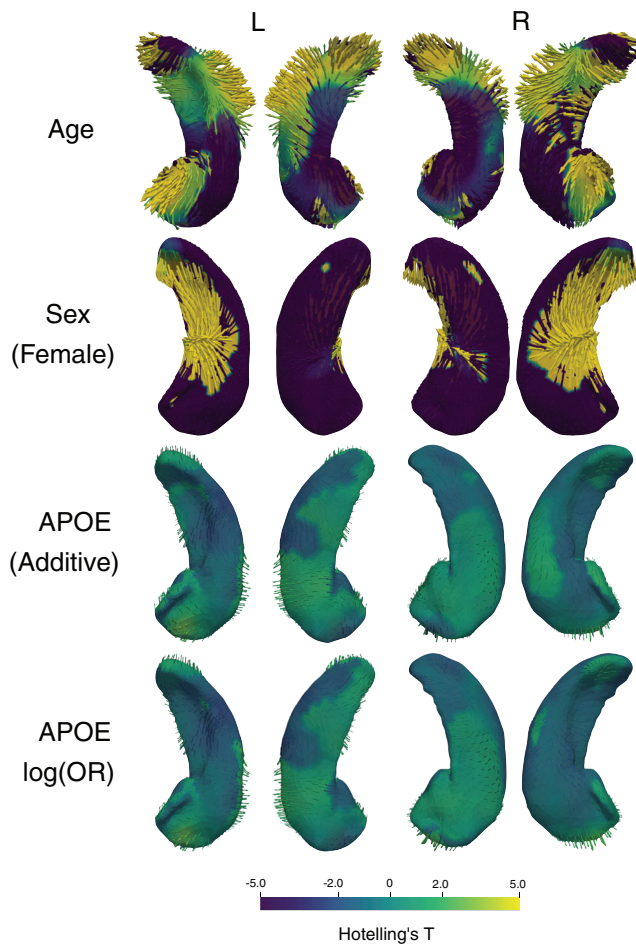


FIGURE 2 Directional effect on the surface of the hippocampus for (from top to bottom) age, sex and APOE: Additive and log(OR) (odds ratio). ALFA cohort with the base model. Positive values (colored in light yellow) indicates expansion. Negative values (colored in dark violet) indicates contraction. Arrow length and size indicate a stronger effect

the magnitude of the vector of the corrected effect with respect to the three peak clusters of the detected region, compared to age, for each of the allele pairs, observing similar interactions depending on the $\epsilon 4$ allele load, with large uncertainty for the $\epsilon 2\epsilon 2$ subjects.

3.2 | ADNI dataset

For the ADNI cohort, after preprocessing (Section 2.2) and discarding subjects with segmentation errors, we ended up with 969 patients. Table S6 shows the ID of all ADNI subjects used in the study.

Table 4 summarizes the main results for all the experiments, using the models described in Section 2.4. “Base model” section shows the effects for age, sex, site, years of education, APOE and DX. Figure 4 shows the effects of selected factors on the surface of both hippocampi. Similar to what happened in ALFA, age and sex present a general contraction over all the surface. DX and APOE also show a general contraction effect. No significant clusters were found on the

effect of acquisition site. “Interactions” section of Table 4 shows results of models with and squared interactions between APOE and age, and between DX and age. For the interaction model between age and diagnosis, no significant clusters were detected. Full results for the interaction model between age and diagnosis and diagnosis and APOE are included in Tables S7 and S8.

On comparison between healthy patients, ADNI includes 256 cognitively healthy patients, with a relatively low proportion of $\epsilon 4$ -homozygotes (6 patients, less than 5%). For this reason, it is difficult to extract meaningful conclusions from the experiments. We tested for main effects and interactions between APOE and age to detect any similarities to the results obtained in ALFA, considering that the obtained results will not have enough statistical power to draw meaningful conclusions. Supporting Information S9 shows the effect on the surface of the hippocampus for APOE and interaction between age and APOE.

4 | SIMILARITY BETWEEN EFFECTS

We quantitatively assessed the similarity between different effects obtained in our tests. Table 5 shows the results for the different selected comparisons. Comparisons 1 to 4 are designed to study similarities between APOE effects and DX effects, whereas comparisons 5 to 8 are aimed to study similar APOE effects across different cohorts. The most relevant comparisons, due to their relevancy or strong effect detected are highlighted in gray and shown in more detail in Figure S10, including the effect maps for both compared effects, the full similarity map, and the significant clusters discovered after the randomization testing (Section 2.5).

shows a comparison between effects of the square additive interaction between age and APOE in ALFA, and the effect of the negative squared interaction between age and diagnosis in ADNI, and the corresponding discovered clusters, observing strong similarities in several regions of the hippocampus for both comparisons. For further results on the similarity tests, Table S11 shows similarities between same effects on different cohorts and Supporting Information S12 and S13 contains the full results for all conducted tests, for the APOE $\epsilon 4$ load models and AD OR model, respectively.

5 | DISCUSSION

In this article, we investigated the effect of APOE $\epsilon 4$ allele load on the surface of the hippocampus. We used multiple linear regression to single out the effect of covariates over the hippocampal surface and analyzed linear and nonlinear interactions between APOE $\epsilon 4$ allele load and age on the hippocampal surface, while taking into account the reduced risk associated with the $\epsilon 2$ allele. We worked with a cohort of cognitively unimpaired subjects with high genetic risk (ALFA). We additionally applied our processing pipeline to a different dataset with subjects at different stages of the disease (ADNI), to study if the interactions and the APOE effect detected in ALFA can be related to the

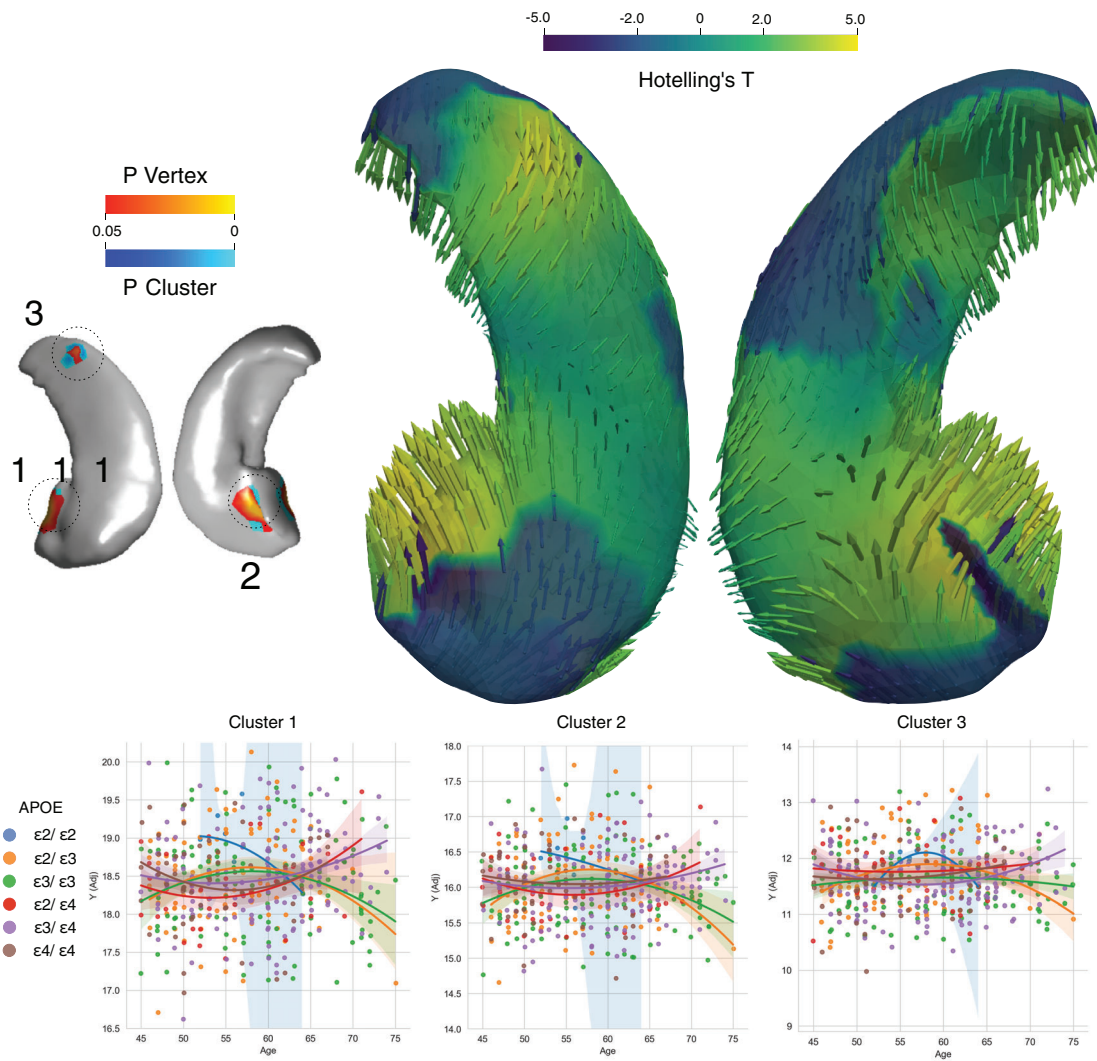


FIGURE 3 Quadratic interaction between APOE OR for AD and age on the right hippocampus after adjusting for other covariates, for all possible allele pairs. Positive values (colored in light yellow) indicates expansion. Negative values (colored in dark violet) indicates contraction. Arrow length and size indicate a stronger effect. For the interaction plots, $Y(\text{adj})$ is the magnitude of the adjusted y variable on the detected cluster. Shaded gray areas indicate 90% confidence intervals

effect of the disease in individuals along the disease continuum. We show some areas of the hippocampus where APOE $\epsilon 4$ effect is comparable to the effect of the disease, suggesting that those regions could be affected in a similar way by APOE before disease onset. To our knowledge, this is the first study that explores interactions between APOE $\epsilon 4$ and age on hippocampal surface using an homozygote enriched dataset of healthy subjects, and compares the result to a dataset of subjects at various stages of the disease.

When adding a linear interaction term to our model for the ALFA dataset between additive APOE effect and age, we detected significant effects (Table 3, linear interaction model) in the CA1 of both hemispheres (Figures S3 and S4).² It is worth noting that this effect, while appearing using a dominant model, is not significant when encoding the AD odds risk model. When adding a squared interaction to the model, APOE OR interactions with age and age squared presented strong effects in the CA1, parasubiculum, and

GC-DG, and on a zone between CA3, CA1, and HATA of the right hippocampus (Figure 3). When observing the interaction in those zones, we see that they are grouped with respect to APOE $\epsilon 4$ allele load (Figure 3, bottom), although the interaction with $\epsilon 2\epsilon 2$ has large uncertainty due to the low number of samples (Table 2). Those results were also observed when using a simpler additive model, although the smallest cluster is not detected (Figure S5). Those areas were also detected when comparing HE to NC. However, dominant and recessive models did not detect significant clusters on those areas.

Findings agree with previous studies on the effect of APOE on hippocampus volume (Cacciaglia et al., 2018; Mueller & Weiner, 2009; Pievani et al., 2011), where strong interactions between APOE $\epsilon 4$ allele load and hippocampal volume on cognitively unimpaired subjects were detected. Going beyond those results, we have been able to suggest specific areas where that interaction is stronger, suggesting

TABLE 4 Results obtained on the ADNI cohort for base, linear interaction, and squared interaction models

	Test	Results			Cluster analysis			
		Hipp	Avg. T	Max. T	N	P_{peak}	$P_{cluster}$	
Base model	Age	R	1.76	13.45	2,379	<.001	<.001	
		L	1.75	14.3	2,185	<.001	<.001	
	Sex	R	2.19	12.85	2,488	<.001	<.001	
		L	2.17	13.73	2,375	<.001	<.001	
	Site	R	0.64	3.60	—	—	—	
		L	0.65	3.24	—	—	—	
	Years ed.	R	0.80	4.33	109	.029	.003	
		L	0.73	4.06	—	—	—	
	APOE (add)	R		0.9	5.1	234	.001	<.001
						144	.013	.003
				1.02	6.38	529	<.001	<.001
	APOE (log(OR))	R		0.92	5.06	476	.002	<.001
						1,223	<.001	<.001
				1.65	11.59	2,289	<.001	<.001
	DX (AD>MCI > CN)	R	1.65	10.10	2,383	<.001	<.001	
		L	1.65	11.59	2,289	<.001	<.001	
	Interactions	APOE (add)×age	R	0.58	3.02	—	—	—
			L	0.68	3.54	—	—	—
APOE (Dom) × age		R	0.6	2.87	—	—	—	
		L	0.72	3.54	—	—	—	
APOE (add) × age ²		R	0.55	3.06	—	—	—	
		L	0.64	3.42	—	—	—	
APOE (Dom) × age ²		R	0.56	2.91	—	—	—	
		L	0.65	3.51	—	—	—	
APOE (log(OR)) × age ²		R	0.54	2.74	—	—	—	
		L	0.6	3.29	—	—	—	
APOE (log(OR)) ² × DX		R	0.65	3.17	—	—	—	
		L	0.7	3.94	—	—	—	
(AD > MCI) × age ²		R	0.71	3.38	—	—	—	
		L	0.75	3.84	—	—	—	

Notes: General test results and information about significant clusters that survived correction are included. Results are divided by model (base, linear interaction or squared interaction). Hipp indicates left (L) or right (R) hippocampus. Max. and Avg. T are the maximum and average Hotelling's T statistic over all vertices, respectively. XX > YY indicates the comparison used for that specific test. For the cluster analysis after correction, N is the number of vertices of the significant cluster. P_{peak} and $P_{cluster}$ are the random field corrected p -values for the peak point and the whole cluster, respectively. Only clusters with $N > 20$ and $P_{cluster} < .05$ are included.

Abbreviations: Add, additive; Dom, dominant; DX, diagnosis; OR, Odds risk; Rec: recessive.

that the way in which age affects hippocampal morphology depends strongly on the APOE allele, something that has also been detected by other researchers (Shi et al., 2014). Such effects can be interpreted as if the interaction between APOE and age is different between hippocampi: there is a linear interaction in both hippocampus, and in the right hippocampus, APOE and age present significant interactions that has less impact at a higher age. Regarding the protective effect of $\epsilon 2$, we could not observe a significant effect on our experiments, given the similarity of the interaction with pairs with and without $\epsilon 2$ and the

uncertainty due to the low amount of $\epsilon 2\epsilon 2$ samples (Figure 3, bottom).

Without introducing interactions in ALFA, APOE does not seem to capture large variations in shape, and indeed, no clusters survived correction (Table 3), in any of the tested APOE models. Subtle differences between APOE groups cannot be easily detected on surface-based studies of the hippocampus, something also observed in other studies with a different cohort of patients (Dong et al., 2019), where such differences were subtle, even before correction. Age presented large

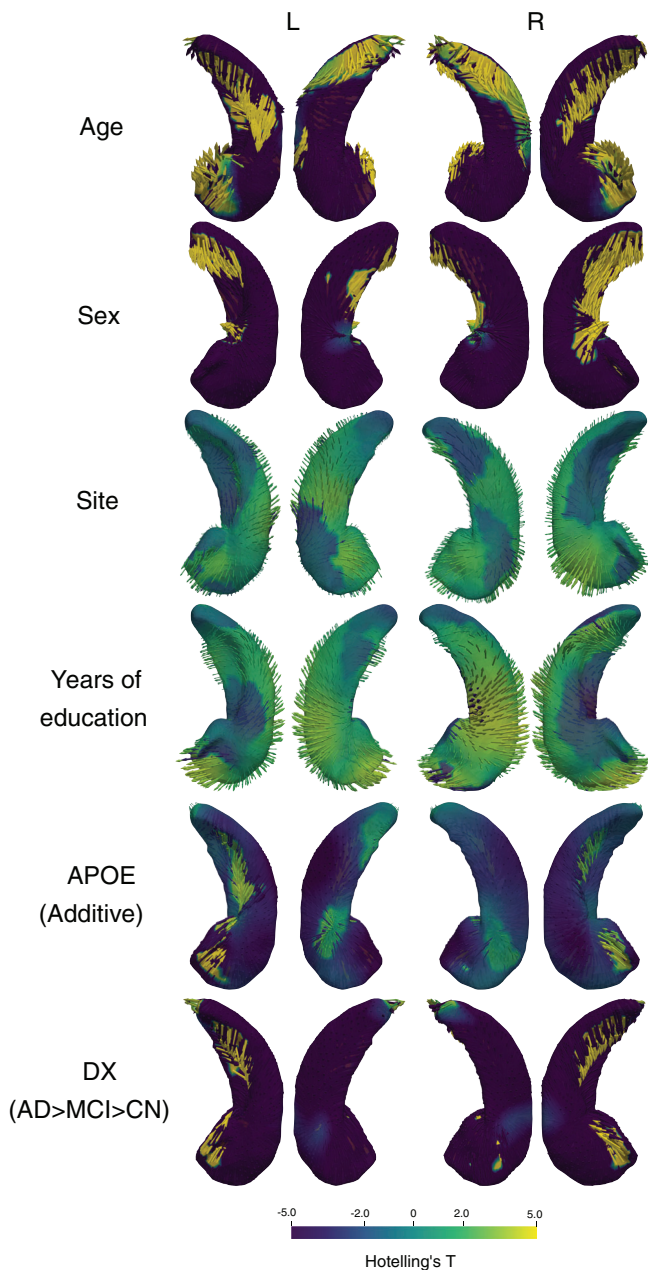


FIGURE 4 Directional effect on the surface of the hippocampus for (from top to bottom) age, sex, site, years of education, APOE and DX. ADNI cohort with the base model. Positive values (colored in light yellow) indicates expansion. Negative values (colored in dark violet) indicates contraction. Arrow length and size indicate a stronger effect

effects over the whole surface, being most of them significant after correction, as shown in Table 3 and Figure 2, an expected result given that age is a known factor affecting hippocampus shape and volume (Lind et al., 2006), and the association between sex and intracranial volume.

Our tests in the ADNI dataset show that the pipeline and the analysis methods are able to capture changes and deformations that agree with current knowledge of the effect that AD has on the hippocampus (Table 4). We observed that age, sex, years of education, and site present significant differences after correction in large regions of

bilateral hippocampi. Differences between AD stages were also strong, showing a general contraction over all the surface of the hippocampus (Figure 4), showing the atrophy caused by the disease. APOE effect also presented a general atrophy effect over all the surface, similar to the AD effect. This similarity can be explained by the unequal distribution of patients for each diagnosis (Table 1), with demented patients having higher APOE based risk. We did not find any significant interactions between APOE $\epsilon 4$ and age in ADNI (Table 4). We did find an interaction between APOE $\epsilon 4$ and DX on the left hippocampus between AD and MCI groups (Table 4), but no other significant results with any other contrasts (Table S8), which suggests that APOE $\epsilon 4$ impacts the three tested stages of AD in a similar way, with a small interaction between MCI and AD. We also tested for interaction between APOE OR and AD diagnosis to see if a protective effect of $\epsilon 2$ could appear, but no significant interaction were found.

Apart from the already mentioned findings on age and APOE interaction on ALFA dataset, we have not detected large differences between our different model encodings of the allele information. Recessive and dominant models did not reveal further zones or interactions that were not already detected by the other models, and additive models (Figure S5) and AD OR models (Figure 3) were the most informative models. Effects maps and results were also very similar between models (Table 3 and Figure 2). This indicates that the effect of APOE $\epsilon 4$ allele load could be modeled more appropriately in a linear (additive) way, or encoding empirical knowledge of the risk to the model (Reiman et al., 2020).

We studied the similarities between APOE $\epsilon 4$ effects and DX effects over ALFA and ADNI cohorts. Results between the same effects (e.g., age vs. age, sex vs. sex) on different cohorts (shown in Table S10) show high similarities, showing that results are comparable between cohorts. Table 5 (comparisons 1–4) show that, for baseline effects, there are some areas on the tail and presubiculum of the hippocampus where a high similarity can be found, with significant clusters detected in the right hippocampus. This could indicate that, even if in our previous tests those regions did not have a strong enough statistical power, APOE $\epsilon 4$ could affect those regions before the onset of the disease, and leave them more vulnerable to the atrophy caused by AD, which is consistent with existing literature on this relationship (Wolk & Dickerson, 2010). However, as previously mentioned, AD and APOE $\epsilon 4$ effects on ADNI (observed in Figure 4) have a general atrophy effect over all the surface, so the found significant areas could simply be regions where APOE produces a contraction effect. We found a large similarity in the interaction effect between squared age and APOE in the ALFA dataset and the inverse interaction effect between squared age and diagnosis in ADNI, with several large significant clusters. This result suggests that age modulates the effect of both APOE and DX over a specific local area on the hippocampal surface in a similar way, being a direct effect for APOE and an inverse effect for DX. Figure 5 shows a larger version of both effect maps, where the similarities between effects can be better appreciated. Similarity is specially high on the right hippocampus, where the interaction between APOE and age in CN subjects is significant (Figure 3). Comparing the similarities obtained using the APOE odds risk model,

TABLE 5 Similarity results between effects

Comparison	Effect 1	Effect 2	Hipp	Sim	N	P
1 ALFA base—ADNI base	APOE (add)	Age	R	0.55	55	.028
			L	0.51	72	.028
	APOE (add)	Years ed.	R	0.61	109	.028
			L	0.56	234	.031
	APOE (add)	APOE (add)	R	0.66	290	.026
			L	0.61	173	.036
	APOE (add)	DX	R	0.62	268	.021
			L	0.58	213	.022
APOE (log(OR))	APOE (log(OR))	R	0.56	79	.022	
		L	0.58	221	.014	
2 ALFA (linear int.)—ADNI base	Age × APOE (add)	DX	R	0.60	239	.025
			L	0.49	96	.020
	Age × APOE (add)	APOE (add)	R	0.57	212	.023
			L	0.54	92	.022
	Age × APOE (Dom)	APOE (Dom)	R	0.59	233	.024
			L	0.51	109	.021
3 ALFA (sq int.)—ADNI base	Age ² × APOE (add)	DX	R	0.50	154	.021
			L	0.62	273	.019
	Age ² × APOE (log(OR))	DX	R	0.60	131	.022
			L	0.63	275	.019
	Age ² × APOE (add)	APOE (add)	R	0.50	187	.023
			L	0.58	240	.019
	Age ² × APOE (Dom)	APOE (Dom)	R	0.50	199	.019
			L	0.53	213	.019
4 ALFA (sq int.)—ADNI (sq int.)	Age ² × APOE (add)	-Age ² × DX	R	0.87	686	.022
			L	0.81	274	.028
	Age ² × APOE (log(OR))	-APOE (log(OR)) × DX	R	0.68	218	.02
			L	0.66	270	.02
5 ALFA base—ADNI NC base	APOE (add)	APOE (add)	R	0.70	169	.026
			L	0.61	201	.023
6 ALFA (sq int.)—ADNI NC(sq int.)	Age ² × APOE (Dom)	Age ² × APOE (Dom)	R	0.53	190	.033
7 ALFA base—ALL base	APOE (add)	DX	L	0.44	35	.021
			R	0.63	260	.021
	APOE (Dom)	APOE (Dom)	L	0.58	206	.024
			R	0.57	155	.030
8 ALFA (sq int)—ALL (sq int)	Age ² × APOE (Dom)	Age ² × APOE (Dom)	L	0.62	135	.036
			R	0.34	—	—
			L	0.36	20	.019

Notes: Hipp indicates left (L) or right (R) hippocampus. Sim is the mean similarity for all vertices. XX > YY indicates the comparison used for that specific test. N is the number of vertices of the significant cluster. P is the mean p-value of the significant cluster. Only the largest detected cluster of each test is included in the table. Only clusters with $N > 20$ and $P_{cluster} < .05$ are included. Rows highlighted are shown in more detail in Figure S10.

Abbreviations: Add, additive; Dom, dominant; DX, diagnosis.

they are very similar to the ones obtained using additive/dominant models, in line with previous observations (Tables 12 and 13).

We tested our methods on a subset of the ADNI dataset, to be able to directly compare two different cohorts of cognitively healthy

patients, and we also did additional analysis by combining both cohorts. Table 5 (comparisons 5 to 8) shows the obtained results. We compared between APOE effects, between APOE and DX effects, and between interactions. Similar areas were found, but the detected significant

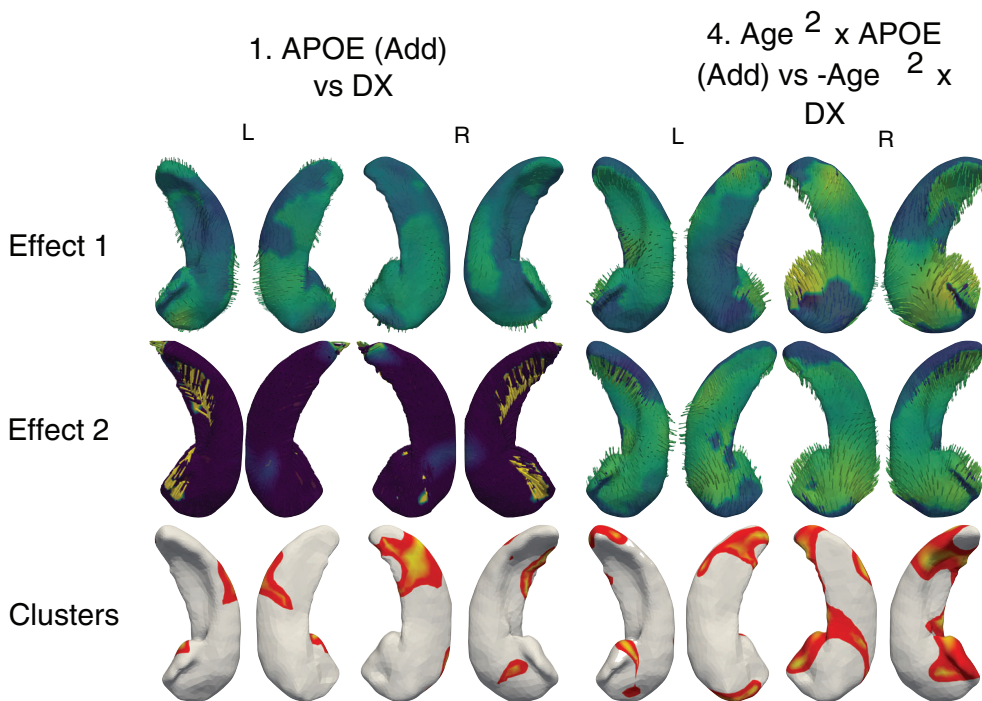


FIGURE 5 Effects of the squared additive interaction between age and APOE in ALFA dataset (above) and the effects of the negative squared interaction between diagnosis and age in ADNI (below). Both hippocampus are represented

clusters are small and nonconclusive. For the combination of cohorts, no significant results were found (Tables S1 and S2 and Figures S14 and S15). This lack of significant results could suggest that the interaction effect detected in ALFA is strongly influenced by the $\epsilon 4$ homozygotes, of which the ADNI cohort has a lower proportion.

We conjecture three (nonexclusive) reasons for the results obtained in those comparisons. First, the site variable for the combined cohort (we added a new category for ALFA subjects) captured much more variation than in previous tests with only ADNI patients, where differences were not significant. This variation shows that differences in image acquisition and protocols between sites greatly influence the obtained MRI and hence the obtained hippocampus mesh. Second, the age disparity between datasets (Figure S16). ADNI individuals are older than ALFA ones, due to differences in study recruitment and aim (ALFA focuses on cognitively healthy subjects, with no signs of the disease, whereas ADNI focuses on subjects that are already in the AD continuum). This difference in the age distribution could also explain why detected interactions in ALFA are not present in ADNI, should such interactions only happen (or be more apparent) at an earlier age. Finally, there could exist other population differences that are not being accounted for.

Our study presents various limitations. First, even if our analysis allows for testing any effect on the surface of the hippocampus, we focused on APOE $\epsilon 4$ allele load and interactions with age. We could add to our analysis other risk factors, such as relevant genotypic factors, cognitive scores, or lifestyle and cardiovascular factors. One key advantage of ADNI over ALFA at this stage is the availability of biomarker status on cerebrospinal fluid. $A\beta$ levels in ADNI could be used to disentangle whether differences observed in ALFA might be due to abnormal amyloid levels or interactions with such levels. However, previous reports have determined that the impact of amyloid accumulation on morphological changes in the brain of cognitively unimpaired individuals is low, a

well as any interactive effects of APOE $\epsilon 4$ (Lim et al., 2017; Liu et al., 2015). For multimodal analysis, methods such as multiple kernel learning, which has been used on other types of medical data for disease characterization, could be used (Martí-Juan, Sanroma, & Piella, 2019; Sanchez-Martinez et al., 2017). Another interesting line of work is to directly study the deformations and effects that happen at the different hippocampus subfields, similar to (Zhao et al., 2019). Second, our analysis was limited to the hippocampus region, but we could extend them to other parts of the brain that present differences in healthy subjects, such as the ventricles. Third, given the large effect of the site in our analysis, segmentation should be improved to ensure robust comparisons between datasets. Moreover, we only used cross-sectional data. Extending our analysis to a longitudinal cohort may allow us to test the shape changes over time, which could also be affected by APOE $\epsilon 4$.

6 | CONCLUSIONS

In this article, we have studied differences in hippocampal surface shape on a cohort of genetically enriched cognitively healthy subjects. We have shown a linear and quadratic interaction between APOE $\epsilon 4$ allele load and age on two different surface regions of the right hippocampus. We have also applied the same method on a different cohort of subjects (including both cognitively impaired and unimpaired subjects), and detecting remarkable similarities between the APOE interaction with age in asymptomatics and the effect of the disease in a second cohort. Results suggest that for late/middle-aged cognitively unimpaired subjects, APOE $\epsilon 4$ exerts an effect on the hippocampal surface comparable to that observed in clinical stages of AD but to a lower extent. In addition, these effects interacted with age, showing a remarkable similarity across the two studied cohorts.

ACKNOWLEDGMENTS

This publication is part of the ALFA study (ALzheimer and FAMilies). The authors would like to express their most sincere gratitude to the ALFA project participants, without whom this research would have not been possible. The project leading to these results has received funding from “la Caixa” Foundation (ID 100010434), under agreement LCF/PR/GN17/50300004. Additional support has been received from the Universities and Research Secretariat, Ministry of Business and Knowledge of the Catalan Government under the grant no. 2017-SGR-892. This work was also partially funded by the Spanish Ministry of Economy and Competitiveness under the María de Maeztu Units of Excellence Programme 525 [MDM-2015-0502]. JDG is supported by the Spanish Ministry of Science, Innovation and Universities—State Research Agency (RYC-2013-13054). Data collection and sharing for this project was funded by the Alzheimer’s Disease Neuroimaging Initiative (ADNI) (National Institutes of Health Grant U01 AG024904) and DOD ADNI (Department of Defense award number W81XWH-12-2-0012). ADNI is funded by the National Institute on Aging, the National Institute of Biomedical Imaging and Bioengineering, and through generous contributions from the following: AbbVie, Alzheimer’s Association; Alzheimer’s Drug Discovery Foundation; Araclon Biotech; BioClinica, Inc.; Biogen; Bristol-Myers Squibb Company; CereSpir, Inc.; Cogstate; Eisai Inc.; Elan Pharmaceuticals, Inc.; Eli Lilly and Company; EuroImmun; F. Hoffmann-La Roche Ltd and its affiliated company Genentech, Inc.; Fujirebio; GE Healthcare; IXICO Ltd.; Janssen Alzheimer Immunotherapy Research & Development, LLC.; Johnson & Johnson Pharmaceutical Research & Development LLC.; Lumosity; Lundbeck; Merck & Co., Inc.; Meso Scale Diagnostics, LLC.; NeuroRx Research; Neurotrack Technologies; Novartis Pharmaceuticals Corporation; Pfizer Inc.; Piramal Imaging; Servier; Takeda Pharmaceutical Company; and Transition Therapeutics. The Canadian Institutes of Health Research is providing funds to support ADNI clinical sites in Canada. Private sector contributions are facilitated by the Foundation for the National Institutes of Health (www.fnih.org). The grantee organization is the Northern California Institute for Research and Education, and the study is coordinated by the Alzheimer’s Therapeutic Research Institute at the University of Southern California. ADNI data are disseminated by the Laboratory for Neuro Imaging at the University of Southern California. Data used in precreation of this article were obtained from the Alzheimer’s Disease Neuroimaging Initiative (ADNI) database (adni.loni.usc.edu). As such, the investigators within the ADNI contributed to the design and implementation of ADNI and/or provided data but did not participate in analysis or writing of this report. A complete listing of ADNI investigators can be found at (http://adni.loni.usc.edu/wp-content/uploads/how_to_apply/ADNI_Acknowledgement_List.pdf).

List of ALFA study collaborators: Eider M. Arenaza-Urquijo, Alba Cañas, Carme Deulofeu, Ruth Dominguez, Karine Fauria, Marta Féllez-Sánchez, José M. González de Echevarri, Xavi Gotsens, Oriol Grau-Rivera, Laura Hernandez, Gema Huesa, Jordi Huguet, Paula Marne, Tania Menchón, Marta Milà-Alomà, Carolina Minguillon, Maria Pascual, Albina Polo, Gonzalo Sánchez-Benavides, Sandra Pradas, Aleix Sala-Vila, Anna Soteras, Marc Suárez-Calvet, Laia Tenas, Marc Vilanova, Natalia Vilor-Tejedor.

DATA AVAILABILITY STATEMENT

Parts of the data that support the findings of this study are available from Alzheimer’s Disease Neuroimaging Initiative (ADNI). Restrictions apply to 685 the availability of these data, which were used under license for this study. Data are available at <http://adni.loni.usc.edu/> upon application. ALFA study data that support the findings of this study are available from the corresponding author upon reasonable request.

ORCID

Gerard Martí-Juan  <https://orcid.org/0000-0003-4729-7182>

Juan Domingo Gispert  <https://orcid.org/0000-0002-6155-0642>

ENDNOTES

¹ <https://github.com/GerardMJuan/hippo-surf-analysis>

² We use the hippocampal subfield map from Iglesias et al. (2015) as reference.

REFERENCES

- Alzheimer’s Association. 2018. “Alzheimer’s Dement: Global Resources.” <https://www.alz.org/global/>.
- Apostolova, L. G., Morra, J. H., Green, A. E., Hwang, K. S., Avedissian, C., Woo, E., et al. (2010). Automated 3D mapping of baseline and 12-month associations between three verbal memory measures and hippocampal atrophy in 490 ADNI subjects. *NeuroImage*, 51(1), 488–499. <https://doi.org/10.1016/j.neuroimage.2009.12.125>
- Avants, B. B., Epstein, C. L., Grossman, M., & Gee, J. C. (2008). Symmetric diffeomorphic image registration with cross-correlation: Evaluating automated labeling of elderly and neurodegenerative brain. *Medical Image Analysis*, 12(1), 26–41. <https://doi.org/10.1016/j.media.2007.06.004>
- Beg, M. F., Miller, M. I., Trounev, A., & Younes, L. (2005). Computing large deformation metric mappings via geodesic flows of diffeomorphisms. *International Journal of Computer Vision*, 61(2), 139–157. <https://doi.org/10.1023/B:VISI.0000043755.93987.a>
- Bouix, S., Jens, C., Pruessner, D. L. C., & Siddiqi, K. (2005). Hippocampal shape analysis using medial surfaces. *NeuroImage*, 25(4), 1077–1089. <https://doi.org/10.1016/j.neuroimage.2004.12.051>
- Bône, A., Colliot, O., & Durrleman, S. (2018). Learning distributions of shape trajectories from longitudinal datasets: A hierarchical model on a manifold of Diffeomorphisms. In *Proceedings of the IEEE Computer Society Conference on Computer Vision and Pattern Recognition* (pp. 9271–9280). New York, NY: IEEE Computer Society.
- Bône, A., Louis, M., Martin, B., & Durrleman, S. (2018). Deformetrica 4: An open-source software for statistical shape analysis. *ShapeMI, Lecture Notes in Computer Science*, 11167, 3–13. <https://doi.org/10.1007/978-3-030-04747-4>
- Cacciaglia, Raffaele, José Luis Molinuevo, Carles Falcón, Anna Brugulat-Serrat, Gonzalo Sánchez-Benavides, Nina Gramunt, Manel Esteller, et al. 2018. “Effects of APOE-ε4 allele load on brain morphology in a cohort of middle-aged healthy individuals with enriched genetic risk for Alzheimer’s disease.” *Alzheimer’s Dement*. 14 (7). Elsevier: 902–12. <https://doi.org/10.1016/j.jalz.2018.01.016>.
- Cates, J., Elhabian, S., & Whitaker, R. (2017). ShapeWorks: Particle-based shape correspondence and visualization software. *Statistical Shape and Deformation Analysis: Methods, Implementation and Applications*, 10, 257–298. <https://doi.org/10.1016/B978-0-12-810493-4.00012-2>
- Chételat, G., & Fouquet, M. (2013). Neuroimaging biomarkers for Alzheimer’s disease in asymptomatic APOE4 carriers. *Revue Neurologique*, 169, 729–736. <https://doi.org/10.1016/j.neuro.2013.07.025>

- Chung, M. K., Worsley, K. J., Nacewicz, B. M., Dalton, K. M., & Davidson, R. J. (2010). General multivariate linear modeling of surface shapes using SurfStat. *NeuroImage*, *53*(2), 491–505. <https://doi.org/10.1016/j.neuroimage.2010.06.032>
- Cong, S., Rizkalla, M., Salama, P., West, J., Risacher, S., Saykin, A., & Li, S. (2015). Surface-based morphometric analysis of hippocampal subfields in mild cognitive impairment and Alzheimer's disease. *IEEE 58th International Symposium on Circuits and Systems (MWSCAS)*, 1–4. Fort Collins, CO: IEEE. <https://doi.org/10.1109/MWSCAS.2015.7282173>
- Costafreda, S. G., Dinov, I. D., Tu, Z., Shi, Y., Liu, C. Y., Kloszewska, I., et al. (2011). Automated hippocampal shape analysis predicts the onset of dementia in mild cognitive impairment. *NeuroImage*, *56*(1), 212–219. <https://doi.org/10.1016/j.neuroimage.2011.01.050>
- Csernansky, J. G., Wang, L., Swank, J., Miller, J. P., Gado, M., McKeel, D., ... Morris, J. C. (2005). Preclinical detection of Alzheimer's disease: Hippocampal shape and volume predict dementia onset in the elderly. *NeuroImage*, *25*(3), 783–792. <https://doi.org/10.1016/j.neuroimage.2004.12.036>
- Cury, C., Durrleman, S., Cash, D. M., Lorenzi, M., Nicholas, J. M., Bocchetta, M., ... Warren, J. (2019). Spatiotemporal analysis for detection of pre-symptomatic shape changes in neurodegenerative diseases: Initial application to the GENFI cohort. *NeuroImage*, *188*, 282–290. <https://doi.org/10.1016/j.neuroimage.2018.11.063>
- Cury, C., Glaunès, J. A., Toro, R., Chupin, M., Schumann, G., Frouin, V., ... Colliot, O. (2018). Statistical shape analysis of large datasets based on Diffeomorphic iterative centroids. *Frontiers in Neuroscience*, *12*, 803. <https://doi.org/10.3389/fnins.2018.00803>
- Dill, Vanderson, Alexandre Rosa Franco, and Márcio Sarroglia Pinho. 2015. "Automated methods for hippocampus segmentation: The evolution and a review of the state of the art." *Neuroinformatics* *13* (2). Springer US: 133–50. <https://doi.org/10.1007/s12021-014-9243-4>.
- Dong, Q., Zhang, W., Wu, J., Li, B., Schron, E. H., McMahon, T., et al. (2019). Applying surface-based hippocampal morphometry to study APOE-E4 allele dose effects in cognitively unimpaired subjects. *NeuroImage: Clinical*, *22*, 101744. <https://doi.org/10.1016/j.nicl.2019.101744>
- Durrleman, S., Prastawa, M., Charon, N., Korenberg, J. R., Joshi, S., Gerig, G., & Trounev, A. (2014). Morphometry of anatomical shape complexes with dense deformations and sparse parameters. *NeuroImage*, *101*, 35–49. <https://doi.org/10.1016/j.neuroimage.2014.06.043>
- Fouquet, M., Besson, F. L., Gonneaud, J., La Joie, R., & Chételat, G. (2014). Imaging brain effects of APOE4 in cognitively Normal individuals across the lifespan. *Neuropsychology Review*, *24*(3), 290–299. <https://doi.org/10.1007/s11065-014-9263-8>
- Fox, N. C., E. K. Warrington, P. A. Freeborough, P. Hartikainen, A. M. Kennedy, J. M. Stevens, and M. N. Rossor. 1996. "Presymptomatic hippocampal atrophy in Alzheimer's disease." *Brain* *119* (6). Narnia: 2001–7. <https://doi.org/10.1093/brain/119.6.2001>.
- Gao, Y., Riklin-Raviv, T., & Bouix, S. (2014). Shape analysis, a field in need of careful validation. *Human Brain Mapping*, *35*(10), 4965–4978. <https://doi.org/10.1002/hbm.22525>
- Genin, E., D. Hannequin, D. Wallon, K. Sleegers, M. Hiltunen, O. Combarros, M. J. Bullido, et al. 2011. "APOE and Alzheimer disease: A major gene with semi-dominant inheritance." *Molecular Psychiatry* *16* (9). 903–7. <https://doi.org/10.1038/mp.2011.52>.
- Goparaju, A., Csecs, I., Morris, A., Kholmovski, E., Marrouche, N., Whitaker, R., & Elhabian, S. (2018). On the evaluation and validation of off-the-shelf statistical shape modeling tools: A clinical application. *ShapeMI, Lectures in Notes of Computer Science*, *11167*, 14–27. https://doi.org/10.1007/978-3-030-04747-4_2
- Gori, P., Colliot, O., Marrakchi-Kacem, L., Worbe, Y., Poupon, C., Hartmann, A., ... Durrleman, S. (2017). A Bayesian framework for joint morphometry of surface and curve meshes in multi-object complexes. *Medical Image Analysis*, *35*, 458–474. <https://doi.org/10.1016/j.media.2016.08.011>
- Gower, J. C. (1975). Generalized procrustes analysis. *Psychometrika*, *40*(1), 33–51. <https://doi.org/10.1007/BF02291478>
- Gutiérrez, L., Gutiérrez-Peña, E., & Mena, R. H. (2019). A Bayesian approach to statistical shape analysis via the projected normal distribution. *Bayesian Analysis*, *14*(2), 427–447. <https://doi.org/10.1214/18-BA1113>
- Hayasaka, S., Phan, K. L., Liberzon, I., Worsley, K. J., & Nichols, T. E. (2004). Nonstationary cluster-size inference with random field and permutation methods. *NeuroImage*, *22*(2), 676–687. <https://doi.org/10.1016/j.neuroimage.2004.01.041>
- Hostage, C. A., Choudhury, K. R., Doraiswamy, P. M., & Petrella, J. R. (2013). Dissecting the gene dose-effects of the APOE ϵ 4 and ϵ 2 alleles on hippocampal volumes in aging and Alzheimer's disease. Edited by John C. S. Breitner. *PLoS One*, *8*(2), e54483. <https://doi.org/10.1371/journal.pone.0054483>
- Hotelling, H. (1931). The generalization of Student's ratio. *Annals of Mathematical Statistics*, *2*(3), 360–378. <https://doi.org/10.1214/aoms/1177732979>
- Hsu, Yu, Y., Schuff, N., Du, A. T., Mark, K., Zhu, X., ... Weiner, M. W. (2002). Comparison of automated and manual MRI volumetry of hippocampus in normal aging and dementia. *Journal of Magnetic Resonance Imaging*, *16*(3), 305–310. <https://doi.org/10.1002/jmri.10163>
- Iglesias, J. E., Augustinack, J. C., Nguyen, K., Player, C. M., Player, A., Wright, M., ... Frosch, M. P. (2015). A computational atlas of the hippocampal formation using ex vivo, ultra-high resolution MRI. *NeuroImage*, *115*, 115–137.
- Inlow, M., Cong, S., Risacher, S. L., West, J., Rizkalla, M., Salama, P., ... Shen, L. (2016). A new statistical image analysis approach and its application to hippocampal morphometry. *Lecture Notes in Computer Science*, *9805*, 302–310. https://doi.org/10.1007/978-3-319-43775-0_27
- Jack, Clifford R., Matt A. Bernstein, Bret J. Borowski, Jeffrey L. Gunter, Nick C. Fox, Paul M. Thompson, Norbert Schuff, et al. 2010. "Update on the magnetic resonance imaging core of the Alzheimer's Disease Neuroimaging Initiative." *Alzheimer's Dement.* *6* (3). Elsevier Inc.: 212–20. <https://doi.org/10.1016/j.jalz.2010.03.004>.
- Joshi, S. H., Xie, Q., Kurtek, S., Srivastava, A., & Laga, H. (2016). Surface shape Morphometry for hippocampal modeling in Alzheimer's disease. In *International Conference on Digital Image Computing: Techniques and Applications DICTA*, Gold Coast, QLD, Australia: IEEE. <https://doi.org/10.1109/DICTA.2016.7797087>
- Kim, J., Valdes-Hernandez, M. D. C., Royle, N. A., & Park, J. (2015). Hippocampal shape modeling based on a progressive template surface deformation and its verification. *IEEE Transactions on Medical Imaging*, *34*(6), 1242–1261. <https://doi.org/10.1109/TMI.2014.2382581>
- Li, J., Gong, Y., & Tang, X. (2017). Hierarchical subcortical sub-regional shape network analysis in Alzheimer's disease. *Neuroscience*, *366*, 70–83. <https://doi.org/10.1016/j.neuroscience.2017.10.011>
- Lim, Yen Ying, Robert Williamson, Simon M. Laws, Victor L. Villemagne, Pierrick Bourgeat, Christopher Fowler, Stephanie Rainey-Smith, et al. 2017. "Effect of APOE genotype on amyloid deposition, brain volume, and memory in cognitively Normal older individuals." *Journal of Alzheimer's Disease*. *58* (4). IOS Press: 1293–1302. <https://doi.org/10.3233/JAD-170072>.
- Lind, Johanna, Anne Larsson, Jonas Persson, Martin Ingvar, Lars-Göran Nilsson, Lars Bäckman, Rolf Adolfsson, et al. 2006. "Reduced hippocampal volume in non-demented carriers of the apolipoprotein ϵ 4: Relation to chronological age and recognition memory." *Neuroscience Letters*. *396* (1). Elsevier: 23–27. <https://doi.org/10.1016/J.NEULET.2005.11.070>.
- Liu, C. C., Kanekiyo, T., Xu, H., & Guojun, B. (2013). Apolipoprotein e and Alzheimer disease: Risk, mechanisms and therapy. *NIH Public Access*, *9*, 106–118. <https://doi.org/10.1038/nrneuro.2012.263>
- Liu, Y., Jin Tai, Y., Wang, H. F., Han, P. R., Tan, C. C., Wang, C., ... Tan, L. (2015). APOE genotype and neuroimaging markers of Alzheimer's

- disease: Systematic review and meta-analysis. *Journal of Neurology, Neurosurgery and Psychiatry*, 86(2), 127–134. <https://doi.org/10.1136/jnnp-2014-307719>
- Lorensen, William E., and Harvey E. Cline. 1987. "Marching cubes: A high resolution 3D surface construction algorithm." *ACM SIGGRAPH Computer Graphics*. 21 (4). New York, NY: ACM Press: 163–69. <https://doi.org/10.1145/37402.37422>.
- Madan, Christopher R., and Elizabeth A. Kensinger. 2017. "Test–retest reliability of brain morphology estimates." *Brain Informatics* 4 (2). 107–21. <https://doi.org/10.1007/s40708-016-0060-4>.
- Martí-Juan, G., Sanroma, G., & Piella, G. (2019). Revealing heterogeneity of brain imaging phenotypes in Alzheimer's disease based on unsupervised clustering of blood marker profiles. *PLoS One*, 14(3), 339614. <https://doi.org/10.1371/journal.pone.0211121>
- Miller, M. I., Tilak Ratnanather, J., Tward, D. J., Brown, T., Lee, D. S., Ketcha, M., et al. (2015). Network neurodegeneration in Alzheimer's disease via MRI based shape diffeomorphometry and high-field atlas. *Frontiers in Bioengineering and Biotechnology*, 3, 54. <https://doi.org/10.3389/fbioe.2015.00054>
- Miller, M. I., Trounev, A., & Younes, L. (2006). Geodesic shooting for computational anatomy. *Journal of Mathematical Imaging and Vision*, 24(2), 209–228. <https://doi.org/10.1007/s10851-005-3624-0>
- Molinuevo, J. L., Gramunt, N., Gisbert, J. D., Fauria, K., Esteller, M., Minguillon, C., et al. (2016). The ALFA project: A research platform to identify early pathophysiological features of Alzheimer's disease. *Alzheimer's & Dementia: Translational Research & Clinical Interventions*, 2 (2), 82–92. <https://doi.org/10.1016/j.trci.2016.02.003>
- Morra, J. H., Tu, Z., Apostolova, L. G., Green, A. E., Avedissian, C., Madsen, S. K., et al. (2009). Automated mapping of hippocampal atrophy in 1-year repeat MRI data from 490 subjects with Alzheimer's disease, mild cognitive impairment, and elderly controls. *NeuroImage*, 45 (1), S3–S15. <https://doi.org/10.1016/j.neuroimage.2008.10.043>
- Mueller, S. G., Schuff, N., Raptentsetsang, S., Elman, J., & Weiner, M. W. (2008). Selective effect of Apo e4 on CA3 and dentate in normal aging and Alzheimer's disease using high resolution MRI at 4T. *NeuroImage*, 42(1), 42–48. <https://doi.org/10.1016/j.neuroimage.2008.04.174>
- Mueller, S. G., & Weiner, M. W. (2009). Selective effect of age, Apo e4, and Alzheimer's disease on hippocampal subfields. *Hippocampus*, 19(6), 558–564. <https://doi.org/10.1002/hipo.20614>
- Mueller, Susanne G, Michael W Weiner, Leon J Thal, Ronald C Petersen, Clifford Jack, William Jagust, John Q Trojanowski, Arthur W Toga, and Laurel Beckett. 2005. "The Alzheimer's disease neuroimaging initiative." <https://doi.org/10.1016/j.nic.2005.09.008>.
- Nitzken, M. J., Casanova, M. F., Gimel'farb, G., Inanc, T., Zurada, J. M., & El-Baz, A. (2014). Shape analysis of the human brain: A brief survey. *IEEE Journal of Biomedical and Health Informatics*, 18(4), 1337–1354. <https://doi.org/10.1109/JBHI.2014.2298139>
- O'Dwyer, Laurence, Franck Lamberton, Silke Matura, Colby Tanner, Monika Scheibe, Julia Miller, Dan Rujescu, David Prvulovic, and Harald Hampel. 2012. "Reduced hippocampal volume in healthy young ApoE4 carriers: An MRI study." Edited by Emmanuel Andreas Stamatakis. *PLoS One* 7 (11). <https://doi.org/10.1371/journal.pone.0048895>, e48895.
- Parker, T. D., Slattery, C. F., Yong, K. X. X., Nicholas, J. M., Paterson, R. W., Foulkes, A. J. M., et al. (2019). Differences in hippocampal subfield volume are seen in phenotypic variants of early onset Alzheimer's disease. *NeuroImage: Clinical*, 21, 101632. <https://doi.org/10.1016/j.nicl.2018.101632>
- Pievani, M., Galluzzi, S., Thompson, P. M., Rasser, P. E., Bonetti, M., & Frisoni, G. B. (2011). APOE4 is associated with greater atrophy of the hippocampal formation in Alzheimer's disease. *NeuroImage*, 55(3), 909–919. <https://doi.org/10.1016/j.neuroimage.2010.12.081>
- Protas, H. D., Chen, K., Langbaum, J. B. S., Fleisher, A. S., Alexander, G. E., Lee, W., et al. (2013). Posterior cingulate glucose metabolism, hippocampal glucose metabolism, and hippocampal volume in cognitively normal, late-middle-aged persons at 3 levels of genetic risk for Alzheimer disease. *JAMA Neurology*, 70(3), 320–325. <https://doi.org/10.1001/2013.jamaneurol.286>
- Qiu, A., Taylor, W. D., Zhao, Z., MacFall, J. R., Miller, M. I., Key, C. R., ... Krishnan, R. (2009). APOE related hippocampal shape alteration in geriatric depression. *NeuroImage*, 44(3), 620–626. <https://doi.org/10.1016/j.neuroimage.2008.10.010>
- Reiman, E. M., Arboleda-Velasquez, J. F., Quiroz, Y. T., Huentelman, M. J., Beach, T. G., Caselli, R. J., et al. (2020). Exceptionally low likelihood of Alzheimer's dementia in APOE2 homozygotes from a 5,000-person neuropathological study. *Nature Communications*, 11(1), 667. <https://doi.org/10.1038/s41467-019-14279-8>
- Reiman, E. M., Chen, K., Alexander, G. E., Caselli, R. J., Bandy, D., Osborne, D., ... Hardy, J. (2005). Correlations between apolipoprotein E 4 gene dose and brain-imaging measurements of regional hypometabolism. *Proceedings of the National Academy of Sciences*, 102 (23), 8299–8302. <https://doi.org/10.1073/pnas.0500579102>
- Reiman, E. M., Chen, K., Liu, X., Bandy, D., Meixiang, Y., Lee, W., et al. (2009). Fibrillar amyloid- β burden in cognitively normal people at 3 levels of genetic risk for Alzheimer's disease. *PNAS*, 106(16), 6820–6825. <https://doi.org/10.1073/pnas.0900345106>
- Sanchez-Martinez, S., Duchateau, N., Erdei, T., Fraser, A. G., Bijnens, B. H., & Piella, G. (2017). Characterization of myocardial motion patterns by unsupervised multiple kernel learning. *Medical Image Analysis*, 35, 70–82. <https://doi.org/10.1016/J.MEDIA.2016.06.007>
- Sanroma, Gerard, Victor Andrea, Qualid M. Benkarim, José V. Manjón, Pierrick Coupé, Oscar Camara, Gemma Piella, and Miguel A. González Ballester. 2017. "Early prediction of Alzheimer's disease with non-local patch-based longitudinal descriptors." In *The series Lecture Notes in Computer Science (LNCS), including its subseries Lecture Notes in Artificial Intelligence (LNAI) and Lecture Notes in Bioinformatics*, 10530 LNCS: 74–81. Springer, Cham. https://doi.org/10.1007/978-3-319-67434-6_9.
- Sanroma, G., Wu, G., Gao, Y., & Shen, D. (2014). Learning to rank atlases for multiple-atlas segmentation. *IEEE Transactions on Medical Imaging*, 33(10), 1939–1953. <https://doi.org/10.1109/TMI.2014.2327516>
- Saunders, A. M., Strittmatter, W. J., Schmechel, D., George-Hyslop, P. H., Pericak-Vance, M. A., Joo, S. H., ... Alberts, M. J. (1993). Association of apolipoprotein E allele epsilon 4 with late-onset familial and sporadic Alzheimer's disease. *Neurology*, 43(8), 1467–1472. <https://doi.org/10.1212/wnl.43.8.1467>
- Shakeri, M., Lombaert, H., Datta, A. N., Oser, N., Létourneau-Guillon, L., Lapointe, L. V., ... Alzheimer's Disease Neuroimaging Initiative. (2016). Statistical shape analysis of subcortical structures using spectral matching. *Computerized Medical Imaging and Graphics*, 52, 58–71. <https://doi.org/10.1016/j.compmedimag.2016.03.001>
- Shen, L., Cong, S., & Inlow, M. (2017). *Statistical shape analysis for brain structures* (1st ed.). Amsterdam, Netherlands: Elsevier. <https://doi.org/10.1016/B978-0-12-810493-4.00016-X>
- Shen, L., Ford, J., Makedon, F., & Saykin, A. (2003). Hippocampal shape analysis: Surface-based representation and classification. *Medical Imaging 2003: Image Processing*, 5032, Washington, D.C.: SPIE. <https://doi.org/10.1117/12.480851>
- Shi, J., Leporé, N., Gutman, B. A., Thompson, P. M., Baxter, L. C., Caselli, R. L., & Wang, Y. (2014). Genetic influence of APOE4 genotype on hippocampal morphometry - an N=725 surface-based ADNI study. *Human Brain Mapping*, 35(8), 3903–3918. <https://doi.org/10.1002/hbm.22447>
- Shi, Y., Thompson, P. M., de Bubicaray, G. I., Rose, S. E., Tu, Z., Dinov, I., & Toga, A. W. (2007). Direct mapping of hippocampal surfaces with intrinsic shape context. *NeuroImage*, 37(3), 792–807. <https://doi.org/10.1016/j.neuroimage.2007.05.016>
- Singh, N., Thomas Fletcher, P., Samuel Preston, J., King, R. D., Marron, J. S., Weiner, M. W., & Joshi, S. (2014). Quantifying anatomical shape variations in neurological disorders. *Medical Image Analysis*, 18(3), 616–633. <https://doi.org/10.1016/j.media.2014.01.001>

- Styner, M., Lieberman, J. A., Pantazis, D., & Gerig, G. (2004). Boundary and medial shape analysis of the hippocampus in schizophrenia. *Medical Image Analysis*, 8(3), 197–203. <https://doi.org/10.1016/j.media.2004.06.004>
- Styner, M., Oguz, I., Shun, X., Brechbühler, C., Pantazis, D., Levitt, J. J., ... Gerig, G. (2006). Framework for the statistical shape analysis of brain structures using SPHARM-PDM. *Insight Journal*, 1071, 242–250.
- Tang, X., Qin, Y., Wu, J., Zhang, M., Zhu, W., & Miller, M. I. (2016). Shape and diffusion tensor imaging based integrative analysis of the hippocampus and the amygdala in Alzheimer's disease. *Magnetic Resonance Imaging*, 34(8), 1087–1099. <https://doi.org/10.1016/j.mri.2016.05.001>
- Kate, T., Mara, E. J. S.-A., Tijms, B. M., Wink, A. M., Clerigue, M., Garcia-Sebastian, M., et al. (2016). Impact of APOE- ϵ 4 and family history of dementia on gray matter atrophy in cognitively healthy middle-aged adults. *Neurobiology Aging*, 38, 14–20. <https://doi.org/10.1016/j.neurobiolaging.2015.10.018>
- Thompson, P. M., Hayashi, K. M., De Zubicaray, G. I., Janke, A. L., Rose, S. E., Semple, J., et al. (2004). Mapping hippocampal and ventricular change in Alzheimer disease. *NeuroImage*, 22(4), 1754–1766. <https://doi.org/10.1016/j.neuroimage.2004.03.040>
- Tondelli, M., Wilcock, G. K., Nichelli, P., de Jager, C. A., Jenkinson, M., & Zamboni, G. (2012). Structural MRI changes detectable up to ten years before clinical Alzheimer's disease. *Neurobiology Aging*, 33(4), 825.e25–825.e36. <https://doi.org/10.1016/j.neurobiolaging.2011.05.018>
- Tuminello, E. R., & Han, S. D. (2011). The apolipoprotein e antagonistic pleiotropy hypothesis: Review and recommendations. *International Journal of Alzheimer's Disease*, 2011, 1–12. <https://doi.org/10.4061/2011/726197>
- Vaillant, M., Qiu, A., Glaunès, J., & Miller, M. I. (2007). Diffeomorphic metric surface mapping in subregion of the superior temporal gyrus. *NeuroImage*, 34(3), 1149–1159. <https://doi.org/10.1016/j.neuroimage.2006.08.053>
- Wang, H., & Yushkevich, P. A. (2013). Multi-atlas segmentation with joint label fusion and corrective learning—An open source implementation. *Frontiers in Neuroinformatics*, 7, 27. <https://doi.org/10.3389/fninf.2013.00027>
- Wolk, D. A., & Dickerson, B. C. (2010). Apolipoprotein E (APOE) genotype has dissociable effects on memory and attentional-executive network function in Alzheimer's disease. *Proceedings of the National Academy of Sciences of the United States of America*, 107(22), 10256–10261. <https://doi.org/10.1073/pnas.1001412107>
- Worsley, K. J., Taylor, J. E., Carbonell, F., Chung, M. K., Duerden, E., Bernhardt, B., ... Evans, A. C. (2009). SurfStat: A Matlab toolbox for the statistical analysis of univariate and multivariate surface and volumetric data using linear mixed effects models and random field theory. *NeuroImage*, 47(July), S102. [https://doi.org/10.1016/S1053-8119\(09\)70882-1](https://doi.org/10.1016/S1053-8119(09)70882-1)
- Younes, L., Albert, M., & Miller, M. I. (2014). Inferring changepoint times of medial temporal lobe morphometric change in preclinical Alzheimer's disease. *NeuroImage: Clinical*, 5, 178–187. <https://doi.org/10.1016/j.nicl.2014.04.009>
- Zhang, M., & Golland, P. (2016). Statistical shape analysis: From landmarks to diffeomorphisms. *Medical Image Analysis*, 33, 155–158. <https://doi.org/10.1016/j.media.2016.06.025>
- Zhao, N., Liu, C.-C., Qiao, W., & Bu, G. (2018). Apolipoprotein E, receptors and modulation of Alzheimer's disease. *Biological Psychiatry*, 83(4), 347–357. <https://doi.org/10.1016/j.biopsych.2017.03.003>
- Zhao, W., Wang, X., Yin, C., He, M., Li, S., & Han, Y. (2019). Trajectories of the hippocampal subfields atrophy in the Alzheimer's disease: A structural imaging study. *Frontiers in Neuroinformatics*, 13(March), 1–9. <https://doi.org/10.3389/fninf.2019.00013>
- Zhao, Z., Taylor, W. D., Styner, M., Steffens, D. C., Krishnan, K. R. R., & MacFall, J. R. (2008). Hippocampus shape analysis and late-life depression. Edited by Bernhard Baune. *PLoS One*, 3(3), e1837. <https://doi.org/10.1371/journal.pone.0001837>

SUPPORTING INFORMATION

Additional supporting information may be found online in the Supporting Information section at the end of this article.

How to cite this article: Martí-Juan G, Sanroma-Guell G, Cacciaglia R, et al. Nonlinear interaction between APOE ϵ 4 allele load and age in the hippocampal surface of cognitively intact individuals. *Hum Brain Mapp*. 2021;42:47–64. <https://doi.org/10.1002/hbm.25202>